An accelerated technique of the tilt performance test of straight axially grooved heat pipes

Valeri Vlassov
INPE - National Institute for Space Research
Av. Dos Astronautas, 1758. São José dos Campos - SP. Brazil.
Phone: 55 (12) 3208-6206
E-mail: valeri.vlassov@inpe.br

[1]Jorge Bertoldo Jr, [2]Ulisses Tadeu Vieira Guedes.
INPE- National Institute for Space Research
Av. Dos Astronautas, 1758. São José dos Campos- SP. Brazil
E-mails: [1]jorge.bertoldo@inpe.br, [2]ulisses.guedes@inpe.br

ABSTRACT

In heat pipe (HP) qualification test the capillary limit should be detected as a function of adverse tilts. Usual technique includes the setting of certain tilts on HP and when following gradual steps in increased heat load. For each pattern either steady state shall be achieved or signals of dry-out shall be detected. This test is time consumed and the precision of maximum heat rate detection depends of interval of power steps. In the axially grooved heat pipe under gravity conditions the dry out point sometimes is not well detectable due to effect of partial drying of upper grooves and eventual artery formed by liquid puddle in bottom grooves. The proposed technique is based on controlled and slow heat pipe rotation in adverse direction under certain heat load. Once the signals of dry-out appear, inertial forces of liquid phase contribute on accelerated drying front retreating from the evaporator toward adiabatic section. This assists the fast local overheating in the dried zone that in its turn allows very clear detection of the dry-out event by the temperature sensors. The developed analytical model qualitatively agrees with experimental curves and aims on understanding all mechanisms involved in this phenomenon.

I. INTRODUCTION

Axially grooved heat pipes (HP) hold long – term permanent importance as the most effective passive devices in the heat transport capability in space applications and thermal stabilization of the satellite structural honeycomb panels. Performance inclination test is the integral part of the HP qualification process for the HP Suppliers and can be also conduced by HP Users as part of the incoming inspection tests. In these tests the capillary limit is detected as a function of the adverse tilt of HP. It is desirable that the test procedure is efficient enough, i.e. provides high precision of the dry out detection on the condition that the testing time is minimal.

The conventional technique includes the investigation of the heat transport limitation under different fixed HP inclinations. It is possible to see in previous works, that the basic procedure implies the detection of maximum heat transport capacity by a stepwise increasing the heat rate input, until the temperature in the evaporator zone starts a sudden increase [7–9]. Conducting such experiments is time/labor consuming and troublesome, since all experimental data must be collected at steady state conditions at each heat load step [8]. The precision to detect the Qmax magnitude depends on the heat load increasing step ΔQ. When a small ΔQ is needed to achieve a desired precision, it causes an excessive testing time for each inclination. At the next inclination angle the process procedure shall be repeated starting from the lowest power.

The ESA HP qualification standard PSS-49 [2] establishes two criterions for the dry out occurrence. First criterion (i) looks rather a convention: the dry out is assumed when the maximal temperature difference over the evaporator zone overpasses 5 degrees. The second (ii)

is related to the evaluation of dependence character of the evaporator – adiabatic temperature difference as a function of the heat load applied: when the linearity is broken, it is assumed that the dry out occurs. Such criteria have drawbacks related to some uncertainty in the exact dry-out detection and the extended testing time needed to achieve the required accuracy. Such the uncertainty may be related to the gravity influence during ground testing. For HP the partial dry-out phenomena may occurs at the upper groves, while at the same time the bottom grooves are flooded with liquid coming form eventual puddle. First, in the evaporator zone, the most external parts of the upper groove (close to end cap) become dried first. However, the bottom grooves are fed with liquid from an eventual puddle inevitably formed at the bottom of the vapor channel along the HP length. The more the upper groves become dry, the more liquid the eventual artery receives. Such behavior is more pronounced for high diameter HPs.

The evolution on data acquisition software and appearance of new high precision inclinometers with digital output make it possible to develop more effective HP tilt performance test method alternative to determine the capillary limits under adverse inclinations. The proposed dynamic test time is lesser than the conventional one, because the power steps and multiple steady – state soaks at each angle that is not needed anymore. At the same time the detection of dry-out instant is more clear than for convention technique due to dynamic acceleration effect

II. MATHEMATICAL MODEL OF DRY-OUT

The purpose of this mathematical model (MM) is to reveal the minimal set of key equations which are able to describe qualitatively the phenomenon of dry-out acceleration during HP slow rotation on the test table.

We consider the evaporator as divided in two thermally coupled zones of variable length, one is dryed (of the length L_{ed}) and second - still primed with liquid (L_{el}), also named as active evaporation zone. For these zones, two HP wall average temperatures T_{el} and T_{ed} are introduced in order to provide a conjugation of the thermal respond to a fast dynamic of liquid movement.

With the test table inclination, the bulk of liquid in the grooves moves towards either the condenser or the evaporator, depending on the angular velocity direction. The most important point of the model is the ability to track the dryout-primed front.

To derive the mass conservation we suppose the dryout-primed front is flat, within the assumption of piston-type model [13]. We also suppose the one-dimensional (1D) axial domination of the liquid flow during dry-out, neglecting the effects of upper grooves partial drying and bottom groove overflooding.

The integral control volume encompasses the liquid contained in all evaporator grooves from evaporator-adiabatic zones division to the dryout point.

During transient, the change of liquid mass in the control volume is equal to the difference between the mass entering and leaving the evaporator control volume, m_{lq}, and the fluid mass evaporated from that volume, m_{ev}. Thus the differential form of the liquid mass balance equation in the entire evaporator is

$$\frac{dm_e}{dt} = \dot{m}_{lq} - \dot{m}_{ev}\,. \tag{1}$$

The components of the equations are

$$m_e = \rho \pi D_v \delta_p \varepsilon_x L_{el}\,, \tag{2}$$

$$\dot{m}_{lq} = \rho u_{lq} \pi D_v \delta_p \varepsilon_x\,, \tag{3}$$

where u_{lq} - velocity of liquid on the evaporator-adiabatic zone division, δ_p and w - hight and width of the rectandular groove, D_v - vapor channel diameter, and ε_x - effective axial porosity of the groove structure, ε_x =w/(w+δ_p).

The evaporative mass flow rate, $\dot{m}_{ev}$, is related to the energy conservation of heat load applied to the active evaporator zone Q_{ev}:

$$Q_{ev} = \lambda \dot{m}_{ev} \tag{4}$$

From another hand, the evaporative heat rate Q_{ev} can be expressed through the heat transfer to the vapor core by introducing, as usual, the effective heat transfer coefficient ("film coefficient") of the evaporation active zone h_e

$$Q_{ev} = h_e \pi D_v \varepsilon_s L_{el} (\overline{T}_{el} - T_v) \tag{5}$$

where ε_s - effective surface porosity of the groove structure, $\varepsilon_s = w/(w+b_w)$, and b_w - the distance between two neighbor grooves.

Substituting 2-5 in 1, the key differential equation for length of primed active zone in the evaporator can be derived:

$$\frac{dL_{el}}{dt} = u_{lq} - \frac{h_e \varepsilon_s}{\lambda \rho \delta_p \varepsilon_x} (\overline{T}_{el} - T_v) L_{el} \tag{6}$$

Last term can be interpreted as an effective evaporative velocity u_{ev}; the physical sense of that magnitude is like if the evaporation were occur only at the dry-out point at the front and not over the entire active area of the evaporator liquid internal surface. By this, the differential equation of the evaporator integral mass balance can be presented in a clear and compact form:

$$\frac{dL_{el}}{dt} = u_{lq} - u_{ev} \tag{7}$$

Equation for axial momentum conservation of liquid can be derived from the usual 1D approach of the momentum balance in a differential control volume of dx length, picked for example, from [13], however modified to account the table rotation:

$$\rho \frac{\partial u_x}{\partial t} + \rho u_x \frac{\partial u_x}{\partial x} = \frac{\partial}{\partial x}\left(\frac{2\sigma Cos\,\theta}{w} \right) - \rho g Sin(\omega t) - \frac{\partial}{\partial x}\left(\Delta P_l + \Delta P_{lv} + \Delta P_v \right) \tag{8}$$

The friction terms include the shear stress between the groove surface and liquid (ΔP_l); shearing effect that results from counterflow of vapor (ΔP_{lv}); and pressure lost in the vapor channel (ΔP_v).

The above momentum equation is derived for a small differential control volume; however to simulate the entire HP liquid bulk movement, spatial integration shall be performed over entire HP length considering entire liquid path as a control volume, having the length L_{lq}. Such integration is possible under the usual assumption that axial liquid velocity changes linearly in primed evaporation section and the condensation zone [14]; therefore, we can perform the integration of momentum conservation along HP axis. Figure 1 explains definition of length of zones.

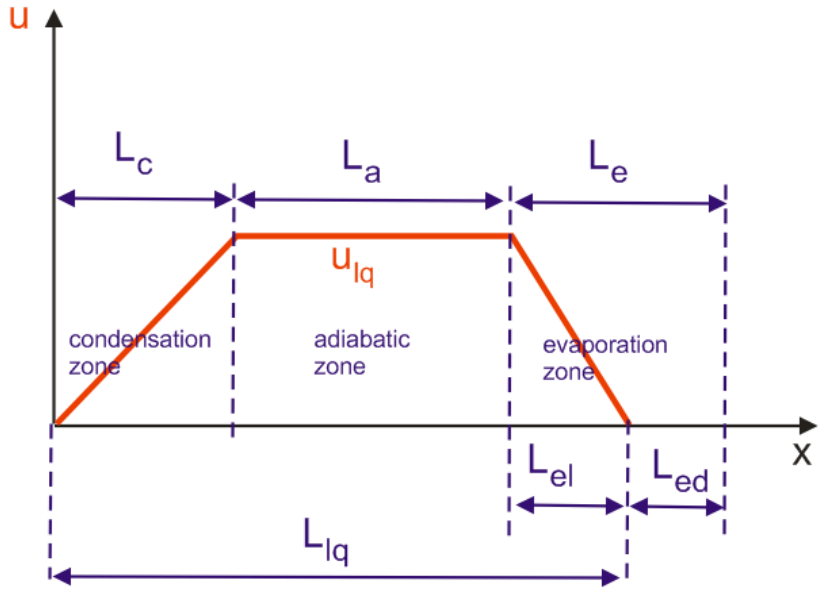

Figure 1. Definition of length of zones and bulk velocity

The integration of the first term of Eq. (8) is performed over entire liquid path and can be separated in the zones of condensation, adiabatic and active evaporation.

$$\int_0^{L_{lq}} \rho \frac{\partial u_x}{\partial t} dx = \int_0^{L_c} \rho \frac{\partial u_x}{\partial t} dx + \int_{L_c}^{L_c+L_a} \rho \frac{\partial u_x}{\partial t} dx + \int_{L_c+L_a}^{L_{lq}} \rho \frac{\partial u_x}{\partial t} dx \tag{9}$$

Third term of the above expression is treated under the assumption of linear axial velocity distribution over the active evaporation zone and the consideration that the active evaporation length L_{el} is a function of time:

$$\begin{aligned} \int_{L_c+L_a}^{L_{lq}} \rho \frac{\partial u_x}{\partial t} dx &= \rho \frac{\partial}{\partial t} \int_{L_c+L_a}^{L_c+L_a+L_{el}} u_x dx = \frac{1}{2} \rho \frac{\partial (u_{lq} L_{el})}{\partial t} = \frac{1}{2} \rho \left(L_{el} \frac{\partial u_{lq}}{\partial t} + u_{lq} \frac{\partial L_{el}}{\partial t} \right) \\ &= \frac{1}{2} \rho \left(L_{el} \frac{\partial u_{lq}}{\partial t} + u_{lq} (u_{lq} - u_{ev}) \right) \end{aligned} \tag{10}$$

Therefore, the first term of the integrated momentum equation is

$$\begin{aligned} \int_0^{L_{lq}} \rho \frac{\partial u_x}{\partial t} dx &= \int_0^{L_c} \rho \frac{\partial u_x}{\partial t} dx + \int_{L_c}^{L_c+L_a} \rho \frac{\partial u_x}{\partial t} dx + \int_{L_c+L_a}^{L_{lq}} \rho \frac{\partial u_x}{\partial t} dx \\ &= \frac{1}{2} \rho L_c \frac{\partial u_{lq}}{\partial t} + \rho L_a \frac{\partial u_{lq}}{\partial t} + \frac{1}{2} \rho \left(L_{el} \frac{\partial u_{lq}}{\partial t} + u_{lq} (u_{lq} - u_{ev}) \right) \\ &= \rho \frac{\partial u_{lq}}{\partial t} L_{eff} + \frac{1}{2} \rho u_{lq} (u_{lq} - u_{ev}) \end{aligned} \tag{11}$$

where

$$L_{eff} = \frac{1}{2} L_{el} + L_a + \frac{1}{2} L_c \tag{12}$$

Integral of the second term of the momentum equation (Eq, 8) vanishes:

$$\int_{L_0}^{L_{lq}} \rho u_x \frac{\partial u_x}{\partial x} dx = \int_{0}^{L_c} \rho u_x \frac{\partial u_x}{\partial x} dx + \int_{L_c}^{L_c+L_a} \rho u_x \frac{\partial u_x}{\partial x} dx + \int_{L_c+L_a}^{L_{lq}} \rho u_x \frac{\partial u_x}{\partial x} dx$$
$$= \frac{1}{2}\rho u_{lq}^2 + 0 - \frac{1}{2}\rho u_{lq}^2 = 0 \tag{13}$$

The capillary pressure gets it maximal magnitude at the dryout point at $x=L_{lq}$; assuming that the capillary pressure changes linearly along axis within each HP zones, even with different inclinations. The integral over the capillary pressure term of Eq. 8 results in

$$\int_{0}^{L_{lq}} \frac{\partial}{\partial x}\left(\frac{2\sigma Cos\,\theta}{w}\right) dx = \frac{2\sigma Cos\,\theta_{\min}}{w} \tag{14}$$

The integral of gravity term is straightforward:

$$\int_{0}^{L_{lq}} \rho g Sin(\omega t) dx = L_{lq}\rho g Sin(\omega t) \tag{15}$$

As friction terms we can use known and well-approved analytical relationships developed in the basic theory for HP pressure lost [9]. For the liquid phase the pressure lost term is derived from the Darcy´s law, accomplished with specific relationships developed for axially grooved capillary structure.

$$\int_{0}^{L_{lq}} \frac{\partial \Delta P_l}{\partial x} dx = \Delta P_l = \mu \frac{u_{lq} L_{eff}}{K} \tag{16}$$

where

$$K = \frac{D_{hp}^2}{2(f\,\mathrm{Re})_l} = \frac{8}{(f\,\mathrm{Re})_l}\left(\frac{\delta_p w}{2\delta_p + w}\right)^2 \tag{17}$$

and by Shah and Bhatti in 1987:

$$(f\,\mathrm{Re})_l = 24\left(1 - 1.3553\left(\frac{w}{\delta_p}\right) + 1.9467\left(\frac{w}{\delta_p}\right)^2 - 1.7012\left(\frac{w}{\delta_p}\right)^3 + 0.9564\left(\frac{w}{\delta_p}\right)^4 - 0.2537\left(\frac{w}{\delta_p}\right)^5\right) \tag{18}$$

The groove basic configuration is shown in Fig. 2

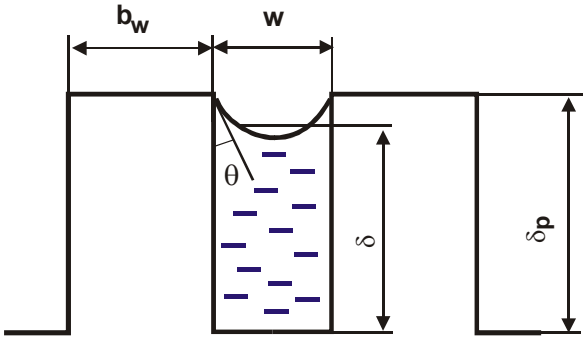

Figure 2. The groove basic configuration

The pressure lost in the vapor channel under assumptions of incompressible, laminar flow and small radial Reynolds number can be expressed as:

$$\int_0^{L_{lq}} \frac{\partial \Delta P_v}{\partial x} dx = \Delta P_v = \frac{128 \mu_v \dot{m}_{ev}}{\pi \rho_v D_v^4} L_{eff} \tag{19}$$

The liquid-vapor frictional interaction is described by the model, given by Schneider and DeVos and recommended by Faghri [9] for rectangular grooves:

$$\int_0^{L_{lq}} \frac{\partial \Delta P_{lv}}{\partial x} dx = \Delta P_{lv} = \frac{\mu_l u_{lq} \psi}{K} L_{eff} \tag{20}$$

where

$$\psi = \frac{w^3}{6(w+b)D_v^2} \cdot (f\,\mathrm{Re})_v \frac{\mu_v \rho_l}{\mu_l \rho_v} \left[1 - 1.971 \cdot \exp\left(-\frac{\pi \delta_p}{w} \right) \right] \tag{21}$$

Present hydraulic part of the model does not account the effects of meniscus curvature change and eventual recession close to dry-out point. Such effects may be reflected in the equations by introducing an adjusting coefficient to account the hydraulic resistance increasing.

Finally, the integrated axial momentum conservation over the entire liquid path is resumed in an ordinary differential equation:

$$\begin{aligned} &\rho \frac{\partial u_{lq}}{\partial t} L_{eff} + \frac{1}{2} \rho u_{lq} (u_{lq} - u_{ev}) = \\ &\frac{2\sigma Cos\,\theta_{\min}}{w} - L_{lq} \rho g Sin(\omega t) - \frac{\mu_l u_{lq} (1+\psi)}{K} L_{eff} - \frac{128 \mu_v \dot{m}_{ev}}{\pi \rho_v D_v^4} L_{eff} \end{aligned} \tag{22}$$

where the liquid path entire length:

$$L_{lq} = L_{el} + L_a + L_c$$

Now we can develop the energy balance part of the MM. As mentioned, we introduce the evaporator as divided in two thermally coupled zones: active, i.e primed with liquid, and in-active, i.e. dried, with its average temperatures T_{el} and T_{ed}. We assume that the applied heat load is distributed homogeneously along the evaporator section. Heat balance equation for the dried zone of the evaporator, when such a zone appears, is expressed as

$$C\rho_w \pi D_w(\delta_w + (1-\varepsilon_x)\delta_p)L_{ed}\frac{d\overline{T}_{ed}}{d\tau} = \left(1-\frac{L_{el}}{L_e}\right)Q - G_{edw}(\overline{T}_{ed} - \overline{T}_{el}) \tag{23}$$

and for the active zone

$$C\rho_w \pi D_w(\delta_w + (1-\varepsilon_x)\delta_p)L_{el}\frac{d\overline{T}_{el}}{d\tau} = \frac{L_{el}}{L_e}Q - h_e \pi D_v \varepsilon_s L_{el}(\overline{T}_{el} - T_v) + G_{edw}(\overline{T}_{ed} - \overline{T}_{el}) \tag{24}$$

Note, due to the dried zone presence, $Q_{ev}<Q$, where Q - is the total heat load applied from a heater to whole evaporator zone.

Effective thermal conductance between two evaporator zones is defined through the distance between the middle points of the zones:

$$G_{edw} = \frac{2k_w \pi(\delta_w + (1-\varepsilon_x)\delta_p)(D_v + \delta_w + (1-\varepsilon_x)\delta_p)}{L_e} \tag{25}$$

Therefore, the developed MM consists of a system of ordinary differential equations, composed by a classical combination of conservation of mass (Eq, 7), momentum (Eq. 22) and energy (Eq. 24-25). The time-dependent variables are: var = $\{T_{el}(t), T_{ed}(t), L_{el}(t), u_{lq}(t)\}$

Any numerical procedure of the integration of the system of ordinary differential equations can be used. The simulations show the model is able to describe qualitatively the phenomenon of dry-out during the dynamic test. The following comparative results show the dry-out development during conventional test (Fig. 3) and dynamic test (Fig. 4):

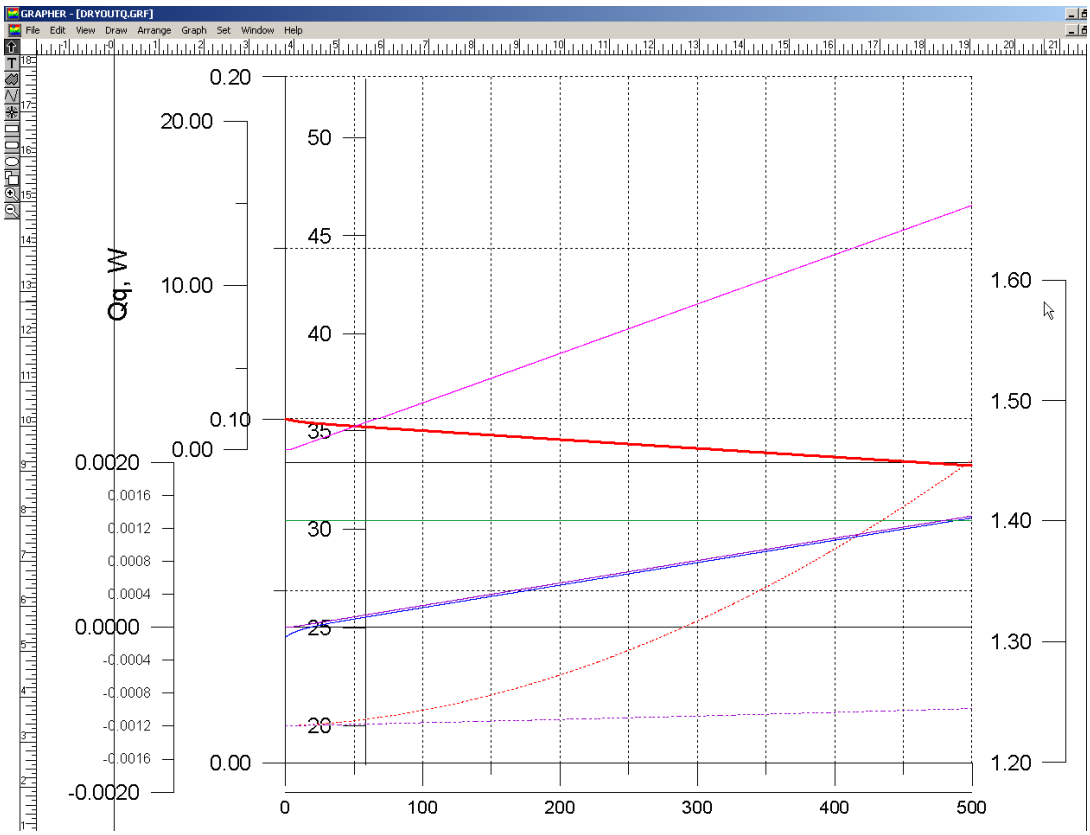

Figure 3. **Result of simulation: dislocation of dryout-primed front and T excursion during conventional test with linear increasing of heat load Q (violet line)**

In Fig.3, that corresponds the conventional technique, the applied heat load was set as a linearly increasing (violet line), while the table inclination was constant (at 1.4 degree, green line). The dry-out front in the evaporator (red line) is moving slowly, retreating from initial position (0.10 m) to final positions (0.08 m) during 500 sec. s a result, the temperature has its corresponding increasing (red dotted line). There is not clear, which instant we could define as a dry out begin.

In Fig 4, that corresponds the dynamic technique, the heat load is set constant, while the table inclination varies from 0 to 1.7 degrees. The dry-out is detected, with some delay, by sudden temperature jump. After this event, operator must change the table rotation direction from adverse to favorable, to prevent overheating. This situation is reproduced in the model (green line). Soon after decreasing the inclination, the liquid return to evaporator and the temperature goes down.

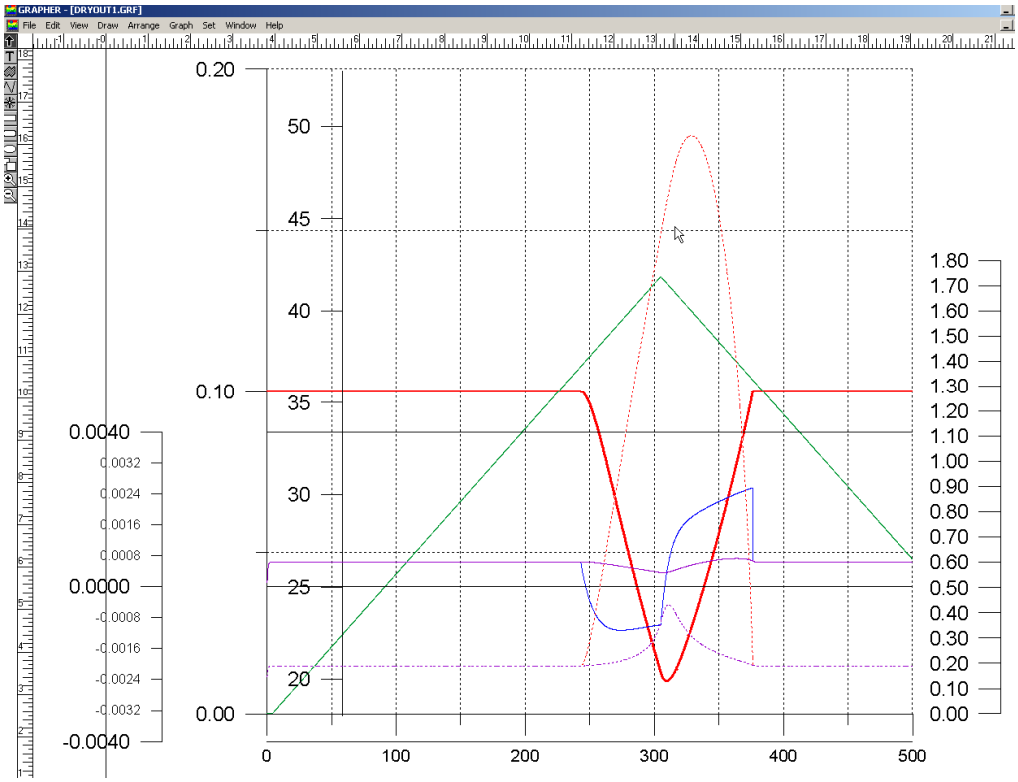

Figure 4. **Result of simulation: dislocation of dryout-primed front (red line) and T jump (red dotted) during dynamic test.**

Therefore the developed MM is able to reveal the acceleration effect on the temperature jump when dry-out occurs during dynamic test. This behavior is very different to one during the conventional test technique.

III. EXPERIMENTAL SET-UP

The heat pipe is a two-core aluminum axially grooved heat pipe filled with ammonia. Such two–core configuration is used in many space applications for structural panel thermal stabilization. The HP profile is 19 x 19 mm of cross section, and its length is 730 mm; each core is 8 mm of effective external diameter and 5.8 mm of vapor channel. The HP profile is extruded from 6063 aluminum alloy, grooves are of trapezoidal; each core consists of 20 grooves. The HP is equipped with two skin heaters and two cooling radiators, as it shown in Fig 5.

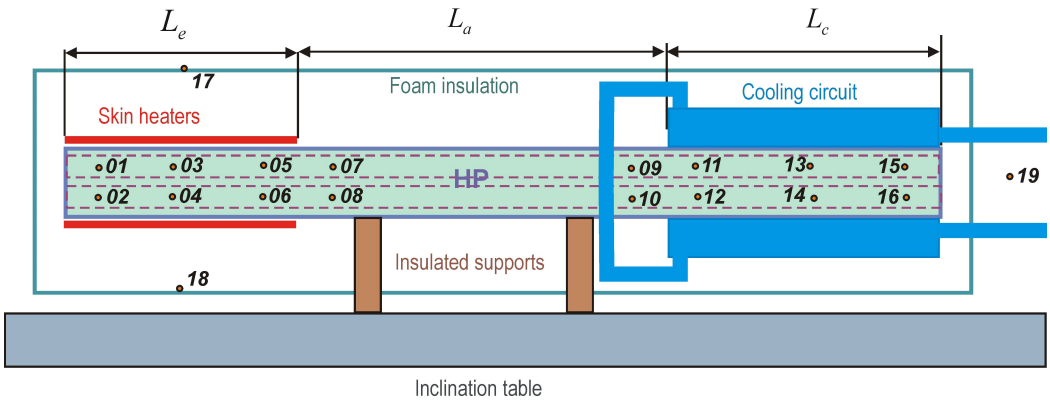

Figure 5. Thermocouples, cooling circuit and skin heaters positioning y

Figure 6 shows the HP cross section and the localization of thermal couples at two cores; the possible liquid puddle formation during ground test is also shown schematically. Upper heating and cooling conditions are provided for the upper core and bottom heating and cooling - for the bottom core simultaneously. Evaporator length is 207 mm (L_e) and condenser length is 180 mm (L_c).

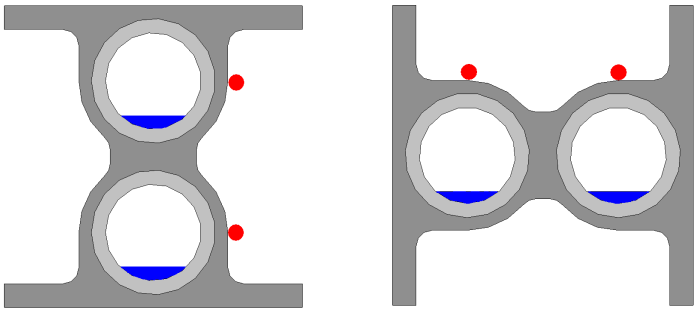

Figure 6. Heat pipe profile and thermocouple location over the cross section

The cross-section shown in Fig. 6 has 20 grooves, 6 mm vapor diameter, 0.8 mm wall thickness, 0.9 mm height grooves, about 0.5 mm width between grooves and about 0.45 mm width grooves. Electrical heaters provide lateral equal heating from both HP sides. The coolant ethylene – glycol circuit yields condenser section cooling controlled by thermostat under volumetric flow rate of 3.3 liter/min.

The instrumentation of the experimental setup includes Agilent Data Acquisition System 34970A, 19 T - type AWG 30 thermocouples, DC Stabilized Power Supply, two MINCO skin heaters HK5285 R3.3L12E and a thermostat Nova Ética to control bath temperature within 1 ^{0}C of precision and 0.1 ^{0}C resolution. The angle is read from Mitutoyo PRO3600 inclinometer giving the angle acquisition within the specified precision of 0.05 degrees and sensitivity of 0.01 degrees. The interval of reading data is 2 sec. The experimental setup is shown schematically in Fig. 7.

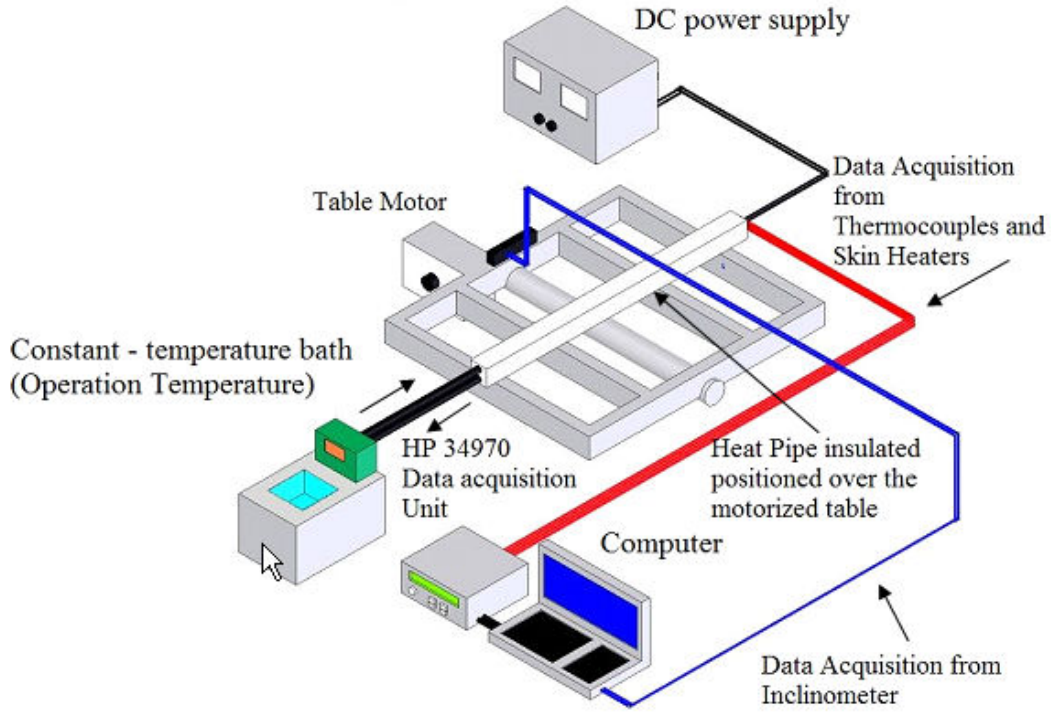

Figure 7. Experimental setup scheme

A digital inclinometer of Mitutoyo has data interface of RS–232C standard. The angle acquisition software was developed in C language, compiled to an executable module for the Windows XP platform. The temperature acquisition and angle acquisition have their time acquisition synchronized.

The motorized table is fabricated with Aluminum profile and equipped with DC motor – reduction gear with an electronic controller which is able to set rotation velocity starting with minimal magnitude of 0.20 deg/min.

Foam insulation is used on the heat pipe to minimize parasitic heat losses or gains from ambient. A separate test was performed to estimate the efficiency of the HP foam insulation. The HP was positioned at unfavorable inclination by 5 degrees to guarantee HP not operates. Then small heat load was applied to the heaters, and the temperature differences were measured under different cooling temperatures. The total average effective thermal resistance of the insulation was extracted from this test and has the magnitude of 0.039 ^{O}C/W.

IV. DYNAMIC DRY-OUT INCLINATION TESTS

The proposed technique of the test basically consists of the following steps. HP is leveled horizontally within the $\pm$ 0.05 degrees precision. Then certain heat load is applied by skin heaters and the cooling system is switched on. After that, HP reaches the steady state heat transfer, the motor is switched on and the heat pipe slowly rotates in adverse inclination. The dry-out is detected through online temperature curve monitoring. Then the temperature curves on the evaporator (Tc01-02) and the condenser zones (Tc11-16) present sudden separation, as Fig. 5 and 6 show, this is considered as the dry out occurrence with clear detection of the instance of the separation combined with the evaporator temperature rise.

After the dry out detection, the table motor shall be promptly switched to inverse its rotation and HP returns to the horizontal position. HP applied heat power is changed to another level and the process is repeated again.

One of peculiarity of the proposed dynamic technique is that the delay on the dery-out detection may depend on the table angular velocity. Several experiment have been performed to define such a dependence. Figure 8 shows the maximum inclination angle, when the dry-out was clearly detected, as a function of table angular velocity. Really, under relative high rotation, the results may be non conservative.

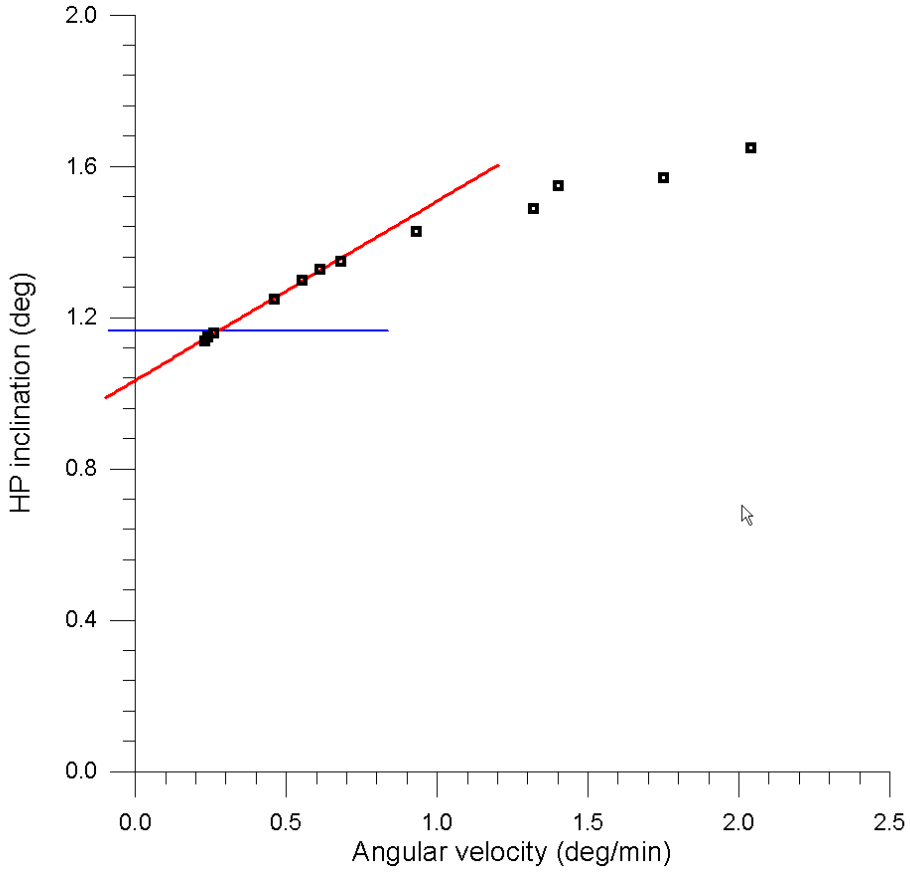

Figure 8. Tilt obtained relative to motorized table velocity rotation

The experimental curve presented near linear character in the region of slow rotations. Therefore the linear extrapolation can be used if velocity is lower than ~1.2 deg/min. Under minimum reachable rotation velocity of 0.23 deg/min the uncertainty in the dry-out angle detection is ~10%, as can be seen from Fig. 8.

If the uncertainty of 10% is not acceptable, two tests shall be performed under different velocities and linear extrapolation shall be applied. The intersection with the Axis at 0-velocity will reveal the exact angle of the dry-out occurrence.

Several experimental data obtained by the dynamic test technique are given in [15]; some results are reproduced below.

Figure 9 shows experimental curve of the dry out occurrence under input heat power of 15 W and cooling circuit temperature of + 20.0 C. The dry out point is clearly identified by sudden evaporation temperatures rise. On this event, condenser temperatures are slightly decreased. The point of the dry out start identifies the exact angle of the event occurrence.

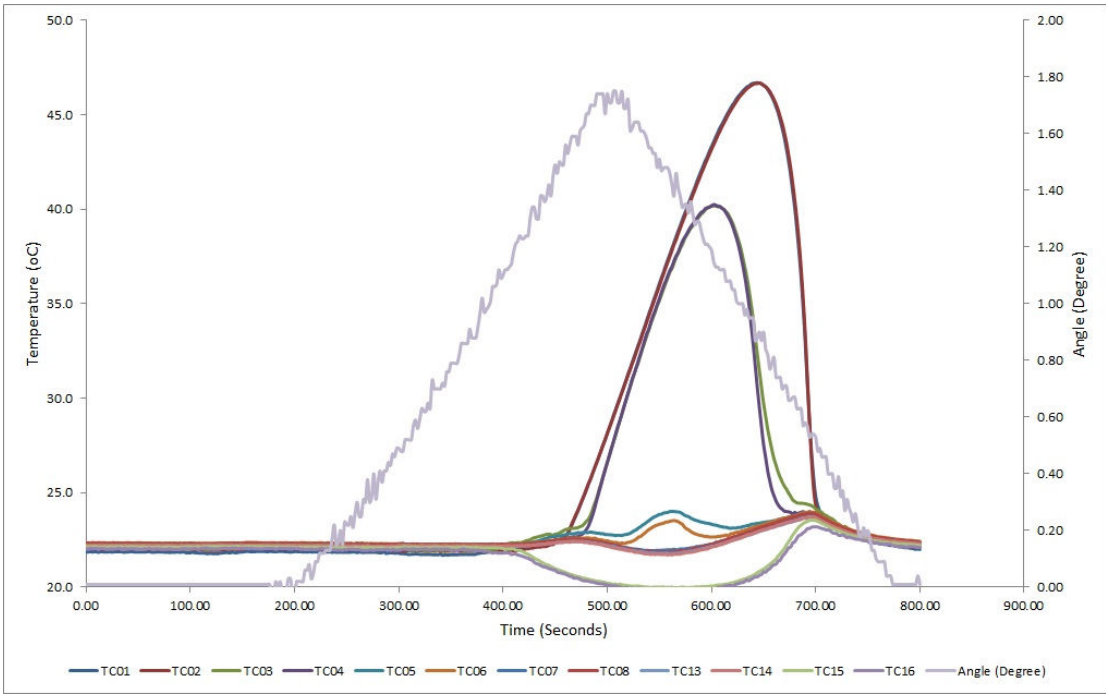

Figure 9. Temperature profiles obtained from the dynamic method

In this figure, the first event occurs on ~250th sec at 1.10 inclination angle. Once the condenser temperature goes down, the eventual liquid puddle displaces to the condenser end and blocks the condensation in the region of 15-16th thermocouples. Probably the entire vapor core in this region gets a blockage, which is confirmed by a registered temperature fall down to the cooling temperature (Tc15 and Tc16 excursions started from 250 sec). The rest of the condenser continues to operate normally: the temperature differences between Tc10 -Tc14 sensors and cooling loop temperature (+20.0 ^{o}C) are kept the same as before the inclination started, however with some slow variations.

Evaporator still continues to operate normally between 250 and 300th sec; a very slight temperature increase is probably related to the reduction of effective area of heat transfer in the condenser due to the liquid blockage in the condenser end region. Straight lines correspond to 0.35 deg/min table rotation. The dry out occurs exactly at 300 sec, when the most-external evaporator temperatures Tc01 and Tc02 get a sudden rise. The inclination angle of the dry-out occurrence is read very precisely. The drying process develops very fast and soon after ~16 sec the dry out front reaches the evaporator middle region (temperatures Tc03 and Tc04 rise).

Considering the distance between sensors Tc01 and Tc03 of 165 mm, the velocity of the dry out front advance can be evaluated as ~ 10.3 mm/sec. After this moment, the rotation of table motor is reversed by the operator, keeping the heat load without changes. With the delay of ~ 14 sec, related to liquid inertia, the temperatures in the middle of evaporator starts to go down, however most external evaporator temperatures (Tc01 and Tc02) still continue to increase. Such opposite tendency lasts about 39 sec, which reveals the estimation of rewetting front recession velocity of 4.2 mm/sec that is more than two times slower than the advancing front velocity.

For the purpose of comparison, several tests were performed following the conventional technique of the capillary limit determination, conducted on the same HP. The certain angle is set, and the power is stepwise increased until the dry out detection. The test results are shown in Fig. 10.

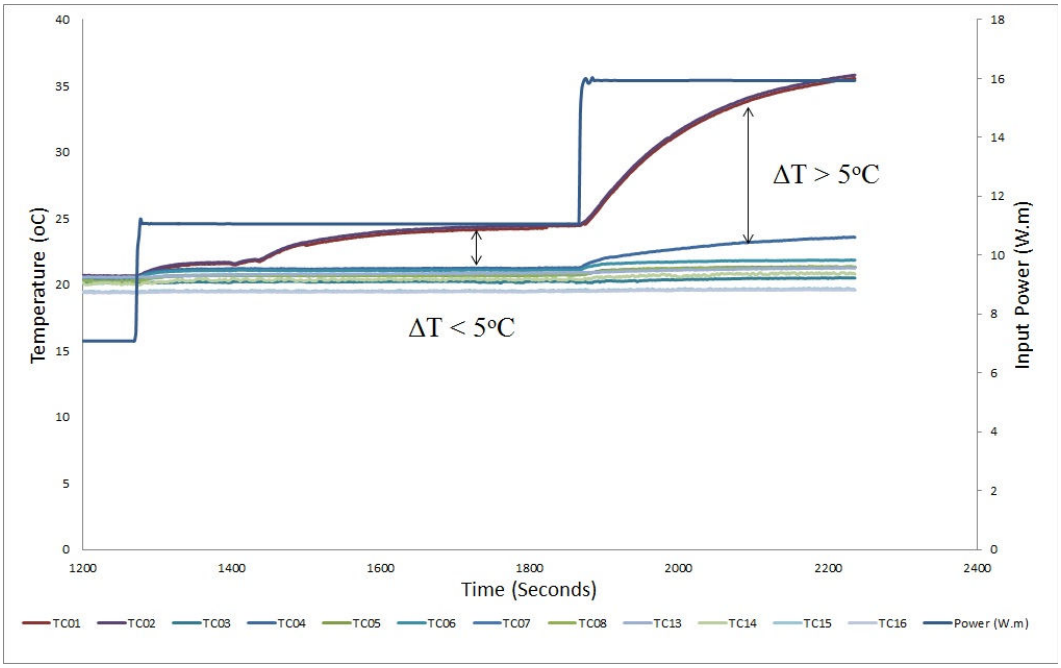

Figure 10. Profile temperatures obtained from the conventional method

The temperature profile is presented for a particular test when the heat pipe positioned in fixed adverse inclination of 1.1 degree and the heat input was increased by 4 W steps. In this example, using the first criterion of $\Delta T < 5^{o}C$ [2], the dry-out is assumed to occur in somewhat between 15 and 22 W. Once the power step of about 4W was used, the uncertainty is about ±16% within the assumption that the criterion is correct. To achieve a better precision, more refined power step interval and more test time are needed.

V. COMPARATIVE RESULTS

Performance inclination tests were conducted by two techniques, conventional and dynamic, under different total heat loads, varied from 15 W up to 135 W, and cooling temperatures varied from -20°C up to 20°C. The comparative results are presented in Fig. 11.

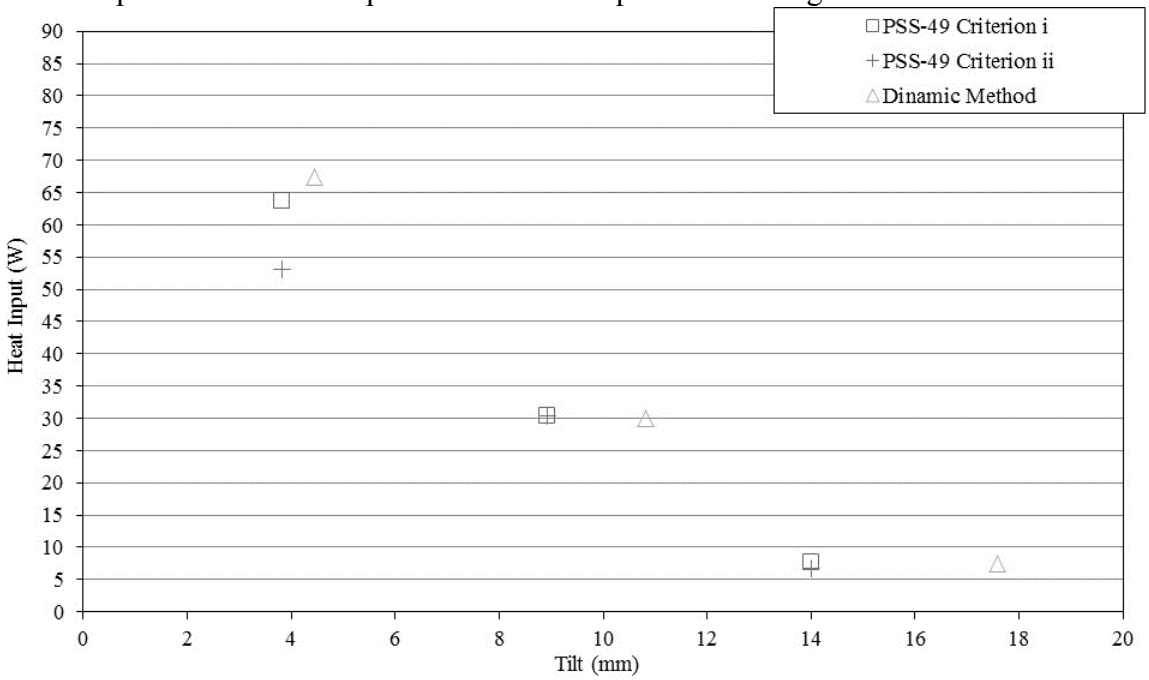

Figure 11. Inclination test results under +20oC of cooling temperature

From the results analysis, it is possible to see that the results obtained from the dynamic method are close to the results obtained from the conventional methods. All results lie within ±26 % of the uncertainty range.

VI. DISCUSSION

The dry out phenomena is primarily a question of the dynamic equilibrium at the liquid – vapor interface, which consists of the balance of different pressures: pressure acting on the interface from the vapor side, pressure acting on the interface from the liquid side, capillary pressure and gravity related pressure. Dry-out front position in the evaporator depends on the mass unbalance between the liquid supply from adiabatic section and the liquid evaporative rate, combined with possible liquid flow momentum and meniscus recession.

In HP horizontal position, the presence of the liquid puddle at the bottom of HP vapor core acts as an eventual artery, which artificially increases the capillary limit. Full dry-out of the evaporator is difficult to occur in this condition; the development of partial dry-out of upper grooves has rather gradual characteristic than sudden; that is why the dry-out phenomenon sometimes is difficult to detect by the convectional technique.

In the low adverse inclinations below ~1 degree, when the puddle still feeds the evaporator zone, this effect of the eventual artery still holds. At higher angles, the puddle artery withdraw from the evaporator zone, however, hydraulic resistance on liquid return from adiabatic zone is kept reduced. In this condition, the HP may operate with partially dried evaporator for a long time when the evaporative rate is balanced with the liquid return supply; the dry-out front does not move forward to the adiabatic zone.

On the hand, during the dynamic test, it was observed that, once the dry-out process begins, the dry-out front starts moving towards the adiabatic zone, and the drying is rapidly developed. It results in temperature rise in dried regions of evaporator, allowing very clear detection of dry-out departing by temperature monitoring. The main reason is that during the dynamic test the liquid bulk gains an additional momentum due to the permanent test table rotation; the magnitude of the momentum is increased due to the permanent increasing of the gravity force component. Such gained acceleration over the liquid bulk breaks the equilibrium between the capillary force and liquid supply because it acts in opposite to the direction of the liquid supplement to evaporator. Dry-out front is not stable anymore and dislocates rapidly towards the adiabatic section; opening grooves get sharp overheating, that clearly detected by temperature sensors.

This increasing gravity assistance on the dry-out development can be considered as an amplification factor of the dry-out phenomenon. Soon after, dried micro-zones get a sudden and clear temperature jump due to the overheating.

The important point in the dynamic test method is the correct choice of the motorized test table angular velocity. Under too slow rotation, it would not be possible to provide the amplification effect of the dry-out development and dry-out front movement that could allow the clear event detection. Under too fast rotation the dry-out instant will be noticed with a certain delay, related to the thermal capacity of HP profile. During this delay, the test table will rotate to a certain angle before the dry-out can be detected by temperature sensors. Therefore, the registered angle will be higher than the real inclination angle when the dry-out really begins. However, as shown in section IV, it can be overcoming by double testing under two different table angular velocities.

VII. CONCLUSIONS

A dynamic test technique is proposed to determine the capillary limits of the aluminum axially-grooved HPs under different adverse tilting. The proposed technique is based on the controlled and constant slow heat pipe inclination in adverse direction under certain heat load

with established steady state conditions. Once the signals of dry-out appear, permanently-increasing gravity force component contributes to the accelerated retreating of the drying front from the evaporator toward adiabatic section. This phenomenon assists the fast overheating development in the dried zone and allows a very clear detection of the dry-out event by temperature sensors. The developed mathematical model confirms qualitatively the mechanism of the acceleration of dry-out development.

This technique allows reducing the testing time necessary to obtain the entire characteristic curve of HP heat transfer capability over the whole range of adverse tilts and to increase the precision of the dry-out moment detection. The comparative results obtained by dynamic and conventional technique are in agreement. According to the authors' opinion, the dynamic test provides more precise and evidence of the dry-out occurrence than the conventional one. The total test time to obtain full characteristic curve is much lesser compared with conventional test methods.

From other hand, the results obtained by the dynamic technique are sensitive to table angular velocity magnitude. Under minimum reachable velocity of 0.23 deg/min the uncertainty in the dry-out angle detection is ~10%. To have very precise results, two tests shall be performed under different velocities and linear extrapolation shall be applied to recalculate the exact angle of the dry-out occurrence.

Besides, the dynamic technique relays on specific requirements to the test equipment and data acquisition software. First, the motorized table shall provide controllable, invertible and very slow constant rotation (about 0.2 deg/min) of the test table. Second, data acquisition software shall provide precise and time-synchronized reading of temperature and inclination angle from digital precise inclinometer. By the author's knowledge, such test setup specifications are still not usual for axial groove HP suppliers for space applications.

ACKNOWLEDGMENTS

The authors would like to thank INPE and LIT for the availability of the laboratory structure and thank all the people who in one way or another contributed to this work. Authors would also like to acknowledge the support of CNPq organization, Brasil, through Research Project 560092/2010-5, Edital MCT/CNPq/AEB 33/2010.

NOMENCLATURE

G = conductance
D = diameter
g = gravity acceleration
L = length
K = permeability
m = mass
$\dot{m}$ = mass flow rate
P = pressure
Q = heat rate
T = temperature
t = time
u = velocity
w = width
x = axial coordinate

δ = groove height
ε = porosity
λ = latent heat

ω = table angular velocity
θ = wetting angle
ρ = density

Subscripts:

a = adiabatic section
c = condenser section
ed = dried evaporator
eff = effective
el = evaporator, primed with liquid
ev = evaporator
s = surface
v = vapor
x = axial

REFERENCES

[1] Z. Lataoui, C. Romestant, D. Petit, Y. Bertin, A. Alexandre, "Heat Pipe Groove Dry Out Front Position Identification using Inverse Methods Analysis", Proceedings of the *14th International Heat Pipe Conference*, Florianopolis, SC, 2007.

[2] "Heat Pipe qualification requirements". ESA PSS –49 Issues 2, March 1983.

[3] G. A. A. Asselman, D. B. Green, "Heat Pipes: I. Operation Characteristics", Philips Technical Review 33 (1973) 103 – 113.

[4] V. Barantsevith, O. Golovin, K. Goncharov, A. Orlov, V. Buz, "Investigation Performance of Axial Grooved Heat Pipes with High Thermal Capacity"*, 12th International Heat Pipe Conference* (12th IHPC), Moscow, 2002.

[5] D. Khrustalev, A. Faghri, "Heat Transfer during Evaporation and Condensation on Capillary – Grooved Structures of Heat Pipes", *ASME Journal of Heat Transfer*, 117 (3) (1995) 740–747.

[6] A. A. El-Nasr, S. M. El – Haggar, Effective thermal conductivity of heat pipes, Heat Mass Transfer 32 (1) (1996) 97–101.

[7] C. A. Busse, J. E. Kemme, Dry – Out Phenomena in Gravity – Assist Heat Pipes with Capillary Flow. *International Journal of Heat Mass and Transfer*, 23 (1980) 643 – 654.

[8] T. E. Tsai, G. W. Wu, C. C. Chang, W. P. Shih, S. L. Chen, "Dynamic test method for determining the thermal performances of heat pipes", *International Journal of Heat and Mass Transfer* 53 (2010) 4567 – 4578.

[9] A. Faghri, "*Heat pipe science and technology*", Taylor & Francis, London, 1995.

[10] "Space engineering: Two – phase heat transport equipment". ECSS – E – ST – 31 – 02C, December 2012.

[11] Z. Lataoui, C. Romestant, Y. Bertin, A. Jemni, D. Petit, "Inverse thermal analysis of the drying zone of the evaporator of an axially grooved heat pipe"*, Experimental Thermal and Fluid Science* 34 (2010) 562–574

[12] G. L. Fleischman, T. C. Cbiang, R. D. Ruff, "Oxigen Heat Pipe 0-G Performance Evaluation Based on 1–G Tests", Proceedings of the *26th AIAA Thermophysics Conference*, 1991.

[13] M. K. Reagan and W. J. Bowman. "Transient Studies of G – Induced Capillary Flow", *Journal of Thermophysics and Heat Transfer* 13 (4) (1999) 537 – 543.

[14] S.W. Chi*, "Heat Pipe Theory and Practice"*, A Sourcebook, Hemisphere Publishing Corporation, 1976.

[15]. J. Bertoldo Junior, Valeri V. Vlassov, G, Genaro, U.T.V. Guedes. "Dynamic Test Method to determine the Capillary Limit of Axially Grooved Heat Pipes". *Experimental Thermal and Fluid Science*. 2014. (To be published).